New Phytologist

Rapid depolarization and cytosolic calcium increase go hand-in-hand in mesophyll cells' ozone response

Maris Nuhkat[1], Mikael Brosché[2], Sonja Stoelzle-Feix[3], Petra Dietrich[4], Rainer Hedrich[5], M. Rob G. Roelfsema[5] and Hannes Kollist[1]

[1]Institute of Technology, University of Tartu, Nooruse 1, Tartu 50411, Estonia; [2]Organismal and Evolutionary Biology Research Program, Faculty of Biological and Environmental Sciences, Viikki Plant Science Centre, University of Helsinki, Viikinkaari 1, Biocentre 3, Helsinki 00790, Finland; [3]Nanion Technologies GmbH, Ganghoferstr 70A, München 80339, Germany; [4]Molecular Plant Physiology, Department of Biology, University of Erlangen-Nürnberg, Staudtstrasse 5, Erlangen 91058, Germany; [5]Molecular Plant Physiology and Biophysics, Julius-von-Sachs Institute for Biosciences, Biocenter, University of Würzburg, Julius-von-Sachs-Platz 2, Würzburg D-97082, Germany

Author for correspondence:
M. Rob G. Roelfsema
Email: roelfsema@botanik.uni-wuerzburg.de

Received: *21 February 2021*
Accepted: *15 August 2021*

New Phytologist (2021) **232:** 1692–1702
doi: 10.1111/nph.17711

Key words: *Arabidopsis thaliana*, Ca^{2+} indicator, Ca^{2+} signalling, membrane depolarization, mesophyll, ozone, reactive oxygen species (ROS).

Summary

- Plant stress signalling involves bursts of reactive oxygen species (ROS), which can be mimicked by the application of acute pulses of ozone. Such ozone-pulses inhibit photosynthesis and trigger stomatal closure in a few minutes, but the signalling that underlies these responses remains largely unknown.
- We measured changes in *Arabidopsis thaliana* gas exchange after treatment with acute pulses of ozone and set up a system for simultaneous measurement of membrane potential and cytosolic calcium with the fluorescent reporter R-GECO1.
- We show that within 1 min, prior to stomatal closure, O_3 triggered a drop in whole-plant CO_2 uptake. Within this early phase, O_3 pulses (200–1000 ppb) elicited simultaneous membrane depolarization and cytosolic calcium increase, whereas these pulses had no long-term effect on either stomatal conductance or photosynthesis. In contrast, pulses of 5000 ppb O_3 induced cell death, systemic Ca^{2+} signals and an irreversible drop in stomatal conductance and photosynthetic capacity.
- We conclude that mesophyll cells respond to ozone in a few seconds by distinct pattern of plasma membrane depolarizations accompanied by an increase in the cytosolic calcium ion (Ca^{2+}) level. These responses became systemic only at very high ozone concentrations. Thus, plants have rapid mechanism to sense and discriminate the strength of ozone signals.

Introduction

Reactive oxygen species (ROS) are important signalling molecules in various plant developmental and stress responses (Mittler, 2017; Waszczak *et al.*, 2018). For example, the superoxide anion ($O_2^{\bullet-}$) and hydrogen peroxide (H_2O_2) form gradients that promote root development, plant immunity, cell death, as well as stomatal movements (Dunand *et al.*, 2007; Tsukagoshi *et al.*, 2010; Kadota *et al.*, 2015; Sierla *et al.*, 2016). The latter response was shown to depend on the leucine-rich-repeat receptor kinase HPCA1, which functions as H_2O_2 sensor in guard cells that activates calcium ion (Ca^{2+}) channels and subsequent stomatal closure (Wu *et al.*, 2020). However, in mesophyll cells the mechanism of ROS perception and the immediate consecutive events are still elusive (Waszczak *et al.*, 2018). Ozone (O_3) degrades into various ROS and elicits a secondary ROS production in plants, the application of O_3 is therefore often used as means for studying ROS-induced processes in plants (Waszczak *et al.*, 2018). Here we use the tropospheric air pollutant O_3 as a proxy to create a burst of apoplastic ROS (Wohlgemuth *et al.*, 2002), to study the earliest steps following ROS perception in mesophyll cells.

Atmospheric O_3 enters plants via stomatal pores and is subsequently absorbed by the apoplastic space of the mesophyll cells, where it can form various ROS, including the hydroxyl radical, $O_2^{\bullet-}$, and H_2O_2 (Grimes *et al.*, 1983; Kanofsky & Sima, 1995; Moldau, 1998; Kollist *et al.*, 2007). Ozone has a high oxidative potential and reacts with various organic substances of the cell wall and the plasma membrane (von Sonntag & Gunten, 2012; Vaultier & Jolivet, 2015). It has been suggested that ROS can damage the function of the plasma membrane by lipid peroxidation, thereby causing a physical disruption and increase of leakiness (Halliwell, 2006; Wong-Ekkabut *et al.*, 2007). In line with the injuries caused by ROS, short high doses of O_3 lead to cell death, while long-term exposure can induce visual lesions (Kangasjärvi *et al.*, 2005; Kadono *et al.*, 2006).

As with many other biotic and abiotic stimuli, an increase of the cytosolic calcium concentration is one of the earliest responses that has been recorded after stimulation with O_3 (Evans *et al.*, 2005; Kadono *et al.*, 2006). Exposure to

70–200 ppb of O_3 for a period of 1 h causes a biphasic calcium response in *Arabidopsis* seedlings as shown by aequorin-based studies: a first transient increase in the calcium level occurs within a minute after the start of the exposure, while the second peak develops slower and is smaller in magnitude (Clayton *et al.*, 1999). The second peak was linked to the upregulation of O_3-responsive genes (Clayton *et al.*, 1999; Short *et al.*, 2012), but the nature and function of the first Ca^{2+} peak has remained unclear.

Several studies indicate that the early O_3-induced Ca^{2+} signals affect ion-transport at the plasma membrane of plant cells. Ozone was shown to decrease the activity of potassium ion (K^+) uptake channels in *Vicia faba* guard cell protoplasts, which are known to be Ca^{2+}-inhibited (Grabov & Blatt, 1999; Torsethaugen *et al.*, 1999), while studies with *Arabidopsis* root cells and cultured cells showed that ROS stimulate the Ca^{2+}-insensitive K^+-efflux channels (Blatt & Armstrong, 1993; Demidchik *et al.*, 2010; Tran *et al.*, 2013). Moreover, very high doses of O_3 (35 000 ppb) applied to *Arabidopsis* cultured cells were reported to induce a fast depolarization, which was linked to the activation of anion channels (Kadono *et al.*, 2010). It is thus likely that O_3 triggers a signalling chain in which the activity of several ion channels is modulated, but the exact sequence of events still needs to be uncovered.

Here we used gas-exchange techniques, membrane potential measurements and a Ca^{2+}-imaging approach to study O_3 responses in leaves. This study revealed that acute doses of O_3, which do not trigger cell death, cause an immediate depolarization of mesophyll cells in three stages that correlate with cytosolic calcium signals.

Materials and Methods

Plant material and growth conditions

The *Arabidopsis thaliana* transgenic plants, expressing the combined R-GECO1-mTurqoise fluorescent Ca^{2+} reporter (from here on RG-mT), were in the Col-0 accession and have been described earlier (Keinath *et al.*, 2015; Waadt *et al.*, 2017). Seeds were vernalized in water at 4°C for 2 d prior to sowing. For gas-exchange experiments the growth substrate consisted of 2 : 1 (w/v) peat : vermiculite. Plants were grown in a Snijders growth chamber (MCA1600; Snijders Scientific, Drogenbos, Belgium), at a 12 h : 12 h day : night cycle at temperature 23°C : 20°C, 150 µmol m^{-2} s^{-1} photon flux density and 70% relative humidity. For the combined membrane potential and calcium imaging experiments, the plants were grown in sterilized soil and grown in a growth chamber (KWBF 720; Binder) at 12 h : 12 h day : night cycle at temperature 21°C : 18°C, 60% relative humidity, with 100 µmol m^{-2} s^{-1} photon flux density. After 12 d, the seedlings were transferred to separate pots and grown for another 3 wk in the same conditions.

Gas-exchange experiments

Gas-exchange experiments were carried out as described previously (Kollist *et al.*, 2007). Briefly, plants were grown through a hole in glass plate covering the pot; the remaining cavity was covered with a bee wax mixture 2 d ahead of the measurements. Experiments were carried out on 24–28 d old plants in a custom-made gas-exchange device with controllable light levels, temperature, and air humidity for intact plants. Conditions in the measurement cuvettes were: 65–75% relative air humidity, ambient CO_2 concentration (*c.* 400 ppm), and a photon flux density 150 µmol m^{-2} s^{-1}. For overnight measurements, eight plants were measured simultaneously and placed to measurement cuvettes the evening before the experiment, at a minimum of 18 h before the onset of O_3. For shorter experiments, all plants were measured separately, and were acclimated for a minimum of 1 h before the start of the experiment, or until the stomatal conductance was stable. For both types of experiments, measurements were averaged over periods of 1 min. Plants were exposed to either 1000 or 5000 ppb of O_3, for 3 or 10 min. All plants in the experiments were used only once.

Electrophysiology

Membrane potential measurements were carried out with leaf discs, which were prepared from 5-wk-old Col-0 plants. First, a leaf was attached with its adaxial side to double-sided adhesive tape in a small Petri dish and cut back to a disc of *c.* 15 × 10 mm. A rubber ring with water repelling lanoline (Sigma-Aldrich, St Louis, MO, USA) was placed on the leaf, while the remaining leaf area was submerged in the following bath solution: 1 mM potassium chloride (KCl), 1 mM calcium chloride ($CaCl_2$) and 1 mM 2-(*N*-morpholino)ethanesulphonic acid (MES), pH 6. In this configuration, the central part of the leaf disc was kept free from the bath solution and thus stayed in direct contact with the atmosphere. The leaf discs were acclimated for a minimum of 1 h in light and then placed on the microscope table. An airflow of 40 l h^{-1} was passed through a humidifier and directed on the liquid-free area of the leaf disc through a stainless-steel dispenser, the position of which remained unchanged throughout the experiment. A constant airflow was maintained for at least 1 h before the leaf disc was exposed to O_3. Ozone was generated with a Certizon (C100; Erwin Sander GmbH, https://www.aqua-sander.de) O_3 generator using an oxygen stream that was added to the main airflow, at the desired concentration using a manostat that was calibrated with a portable O_3 monitor (Series 500; Aeroqual, www.aeroqual.com). In control experiments, the same flow of oxygen was added to the main airflow.

Membrane potential measurements were carried out with a custom-made amplifier (input impedance > 10^{11} Ω, Ulliclamp01) that was connected to microelectrodes via silver/silver chloride half cells. For reference electrode, a glass capillary filled with 300 mM KCl with a 2% agarose 300 mM KCl plug was used, which was placed in the bath solution surrounding the leaf disc. Measurement electrodes were produced from borosilicate glass capillaries (inner diameter, 0.58 mm; outer diameter, 1.0 mm; Hilgenberg, www.hilgenberg-gmbh.com) on a laser puller (P2000; Sutter Instruments Co., www.sutter.com). The electrodes were moved to the cell through open stomata by a piezo

micromanipulator (MM3A; Kleindiek Nanotechnik, www.nanotechnik.com) and the impalement of mesophyll cells was characterized by a sudden change of the measured potential to values ranging from −140 to −200 mV. All O_3 treatment experiments were carried out on different leaf discs, one plant was used to prepare a maximum of two leaf discs.

Patch-clamp recordings were made in the cell-attached configuration, using mesophyll protoplasts enzymatically isolated from 3 to 10-wk-old Col-0 *Arabidopsis* leaves, as described previously (Stoelzle *et al.*, 2003). Sealing procedure was done under white light provided by the microscope halogen lamp (10 µmol m^{-2} s^{-1}). After establishment of the cell-attached configuration the microscope light was turned off to prevent light-activation of cation channels (Stoelzle *et al.*, 2003). Currents were measured by an EPC-9 patch-clamp amplifier (Heka Electronics, www.heka.com) in 1 s voltage ramps, and the current responses were averaged from 10 consecutive ramps applied with an interval of 3 s. Steady-state current amplitudes were determined at the end of 800 ms voltage pulses. The bath solution was composed of 40 mM calcium gluconate and 10 mM MES, pH 5.6 (Tris), the pipette solution contained 10 mM barium gluconate, 4 mM KCl, 4 mM ethylene glycol-bis(β-aminoethyl ether)-*N,N,N′,N′*-tetraacetic acid (EGTA), and 10 mM 4-(2-hydroxyethyl)-1-piperazineethanesulphonic acid (HEPES), pH 7.1 (Tris). Solutions were adjusted to 400 mosm kg^{-1}, using D-sorbitol.

Fluorescence microscopy

Cytosolic [Ca^{2+}] signals were monitored with the fluorescent R-GECO1-mTurquoise reporter protein (Waadt *et al.*, 2017). The fluorescence was recorded using the filter wheels of a spinning disc system (CARV II; Crest Optics, www.crestopt.com) mounted to the fluorescence port of the upright microscope (Axioskop 2FS; Zeiss, www.zeiss.com/microscopy/int/home.html). Light from a light emitting diode (LED) system (pE-4000; CoolLED, www.coolled.com/) at 435 and 580 nm, for mTurquoise and R-GECO1, respectively, was used for excitation. Emission light was passed through dichroic mirrors with cut-off wavelengths of 450 nm (T450 LPXR; Chroma Technology Corp., www.chroma.com) and 590 nm (FF593 BrightLine; Semrock Inc., www.semrock.com) and filtered with band pass filters at 475/28 nm (BrightLine HC; Semrock) and 628/40 nm (BrightLine; Semrock). The excitation light was focused on the specimen with a low-magnification objective (Achrostigmat 5X; Zeiss) and images were captured with an exposure time of 200 ms and an interval of 2 s with a charge multiplying charge-coupled device (CCD) camera (QuantEM; Photometrics, www.photometrics.com). Camera, spinning disc and LED light systems were operated with the VisiView software (Visitron, www.visitron.de).

All fluorescence microscopy experiments were performed on leaf discs, prepared as described earlier. Each leaf disc was used for an experiment only once. For experiments with 5000 ppb O_3, a slice of 1% agarose gel (w/v in water) *c.* 2–3 mm thick and with 1 cm^2 surface area was placed on half of the field of view to reduce the flow of O_3 reaching the leaf surface. The agarose gel covered roughly half of the field of view and reduced the flow of O_3 reaching the leaf surface to less than 0.5% (Supporting Information Fig. S1).

Images were analysed with ImageJ software (Schneider *et al.*, 2012) utilizing NucMed look-up-tables (J.A. Parker, https://imagej.nih.gov/ij/download/luts/) and Time Series Analyzer V3 plugin (Department of Neurobiology, University of California, Los Angeles, CA, USA; https://imagej.nih.gov/ij/plugins/time-series.html). The analysis of fluorescence intensity in veins and/or intercostal areas was conducted for regions of interest (ROIs) that are indicated in the respective figures. For measurements in which 5000 ppb O_3 was applied, the parts of field of view that were in direct contact with the air or covered by the agarose gel were selected for the analysis; for image analysis procedures the whole field of view was used, while the margins of the image were excluded.

Statistical analysis

Repeated measures ANOVA with Tukey *post hoc* test was used to compare before and after O_3 treatment values for stomatal conductance and CO_2 assimilation values as well as membrane potential changes. Statistical analyses were performed with Statistica (v.7.1) software (StatSoft Inc., https://www.statistica.com/en/).

Results

Ozone inhibits CO_2-assimilation before it induces stomatal closure

Whole rosettes of intact *Arabidopsis thaliana* plants were exposed to 3- or 10-min O_3 pulses of 1000 ppb. These O_3 pulses triggered a rapid transient decrease in stomatal conductance (63% lower than the initial value 10 min after O_3 exposure, Fig. 1a), as reported earlier (Kollist *et al.*, 2007; Vahisalu *et al.*, 2010). While the initial responses to 3- and 10-min pulses of O_3 were very similar, later changes in stomatal conductance (the period of 2–6 h after stimulus application) differed considerably (Fig. 1a). After a 3 min O_3 exposure, the plants recovered to a stomatal conductance that was slightly higher than in the control, while a 10 min O_3 exposure caused some recovery but thereafter stomatal conductance remained lower than that of control plants (Fig. 1a). During the night, the stomata closed irrespective of the O_3 treatment, but plants treated with a 3-min O_3 pulse retained a higher stomatal conductance throughout the night. At the end of the 24 h measurements no significant difference in the stomatal conductance was any longer observed.

In contrast to the large changes in stomatal conductance, O_3 provoked only a small decrease in CO_2 assimilation (Fig. 1a). On average, the CO_2 uptake rate was reduced by 15% (16-min time point). Just as the transpiration, the assimilation returned to the same level as control after the dark period (Fig. 1a,b). No visible injury was caused by these O_3 doses (Fig. S2a), which indicates that even the 10 min exposure to 1000 ppb O_3 does not lead to irreversible damage in *Arabidopsis*.

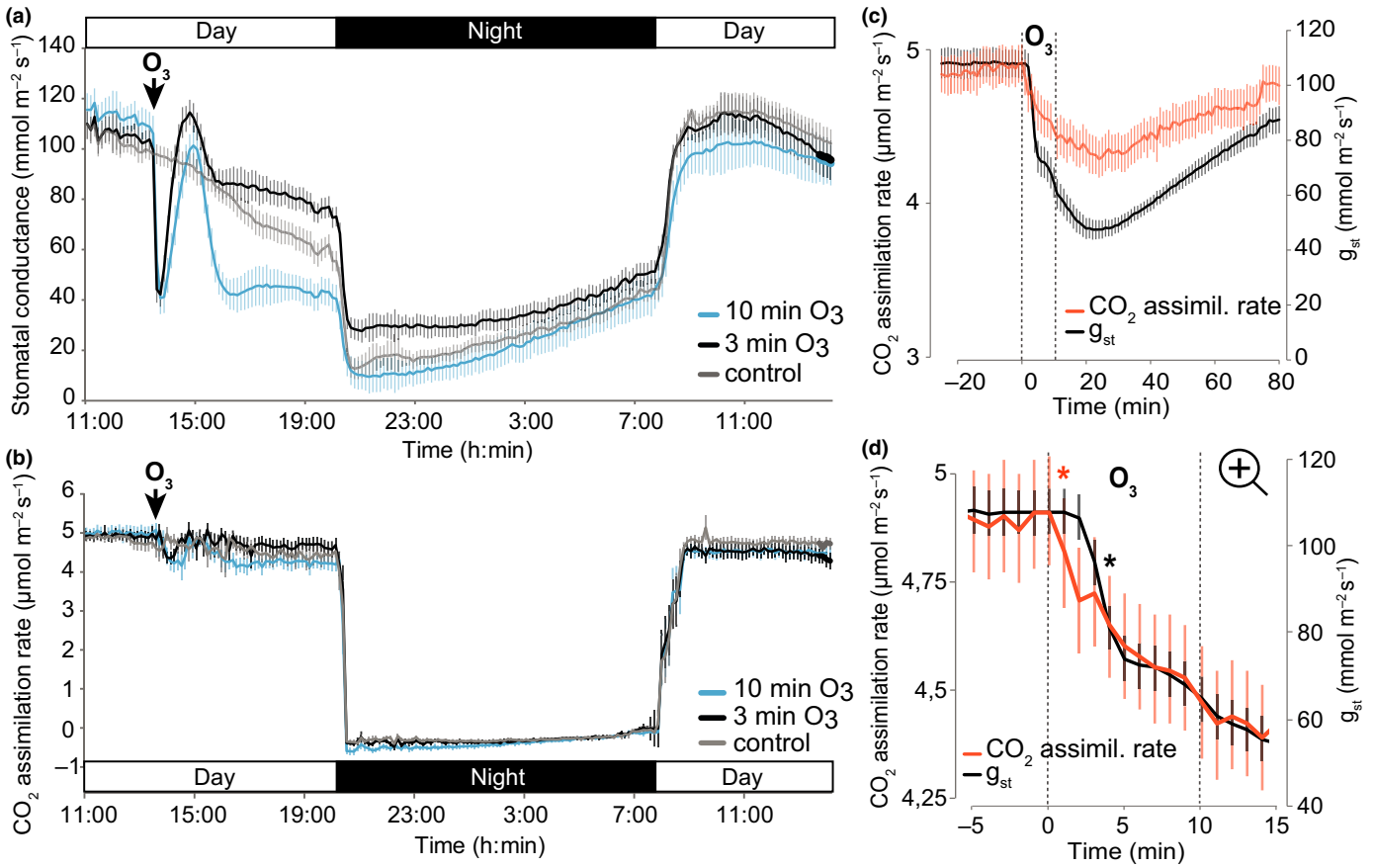

Fig. 1 Stomatal conductance and CO_2 assimilation of 4-wk-old *Arabidopsis thaliana* plants in response to ozone (O_3). Ozone (1000 ppb) was applied for 3 or 10 min (arrow above the traces) and the stomatal conductance (a) and CO_2 uptake rate (b) were recorded for 24 h. Results pooled from three independent experiments are shown, $n = 9$–11, error bars represent SEM. (c, d) Ozone was applied for 10 min and the CO_2 exchange rate was measured at 1 min intervals. The O_3 exposure was started at time point 0, the dashed lines indicate the duration of O_3 treatment. (d) Shows same data as (c) but zooms in at the first minutes after O_3 application. Note that the *y*-axis in (d) also differs from (c). One plant was measured per experiment. An asterisk represents the first statistically significant timepoint during treatment compared to average of last 5 min value before treatment (Tukey HSD, $P < 0.05$). $n = 25$, error bars represent SEM.

The early responses to 10-min O_3 pulses were studied in further detail, by recording the stomatal conductance and CO_2 uptake rate at a 1-min interval (Fig. 1c,d). In line with the experiments described earlier, the stomatal conductance response was much stronger than the change in CO_2 assimilation (Fig. 1c). However, O_3 caused a statistically significant drop in CO_2 assimilation already 1 min after the start of the O_3 exposure ($P = 0.0087$, Tukey honestly significant difference (HSD)), whereas the decrease in stomatal conductance only occurred after 3 min (Fig. 1d). Apparently, O_3 application triggers early processes in mesophyll cells that lead to reduction of photosynthetic CO_2 uptake.

Ozone triggers rapid plasma membrane depolarization in mesophyll cells

The observed early change in the CO_2 assimilation suggested that there is a rapid O_3-induced response in mesophyll cells that precedes the stomatal response. As membrane potential changes often occur in an early stage during stress responses (El-Maarouf *et al.*, 2001; Wendehenne *et al.*, 2002; Colcombet *et al.*, 2009; Jeworutzki *et al.*, 2010) we set up an experimental approach to measure mesophyll plasma membrane responses to application of O_3: *Arabidopsis* leaf discs were submerged in bath solution, but an area in the centre was in direct contact with the atmosphere and could be exposed to O_3 (Fig. 2a). At the start of the experiment, the microscope lamp was turned off, which induced a short hyperpolarization followed by a transient depolarization (Fig. 2b, c; Table S1). Switching light on first triggered a depolarization that was followed by a transient hyperpolarization and a return to an average membrane potential of −168 mV (SEM = 4), in a similar fashion as described earlier (Elzenga *et al.*, 1995). A 3-min O_3 pulse transiently depolarized the mesophyll cells and in a few minutes the membrane potential returned to the pre-stimulus value (Fig. 2b; Table S1). In contrast the mesophyll cells remained depolarized or depolarized even further for at least 30 min after exposure to O_3 for 10 min ($\Delta V = 48$ mV compared to V_m before exposure, SEM = 10.2, $n = 8$). After the 10 min O_3 treatment, the depolarized cells still responded to offset and onset of light (Fig. 2c), but the magnitude of the membrane potential

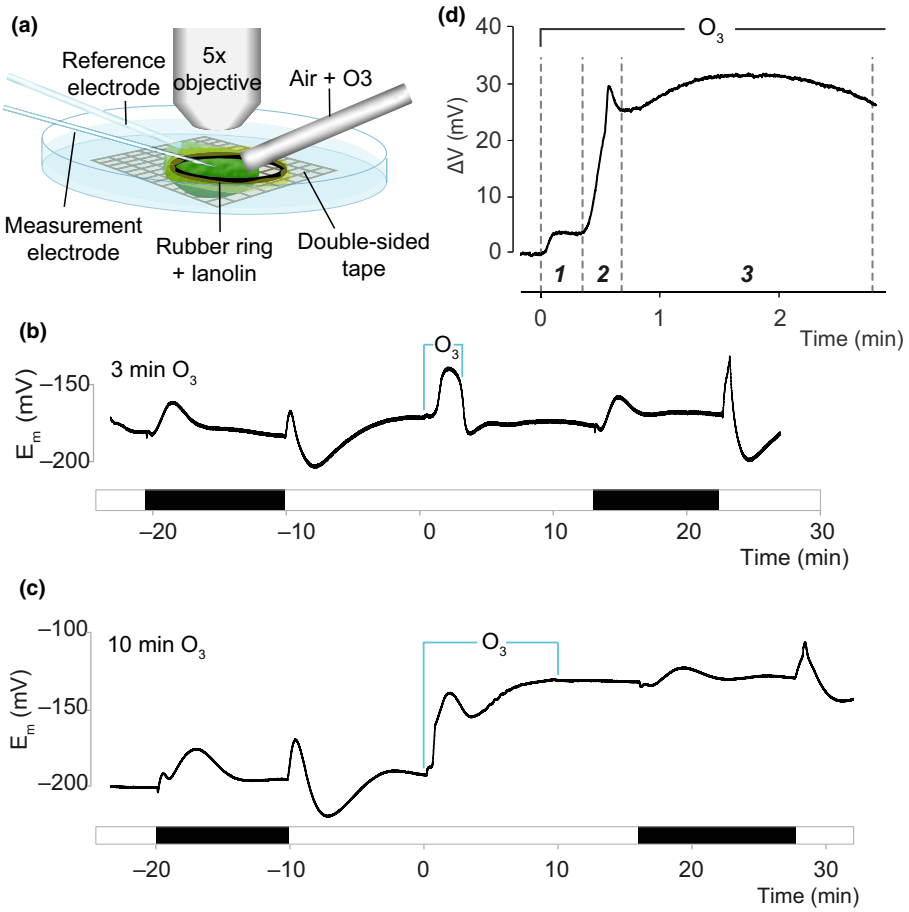

Fig. 2 Ozone (O_3)-induced changes in the membrane potential of *Arabidopsis* mesophyll cells. (a) Drawing of the experimental setup that was used to record the membrane potential response of mesophyll cells to O_3. A leaf disc was attached to double-sided adhesive tape in a small Petri dish and a rubber ring with lanolin was placed on top of the disc; the Petri dish was filled with bath solution, except for the area within the rubber ring. An air flow was directed via a stainless-steel tube onto the solution-free area and O_3 was applied via this air stream. A measurement electrode was inserted into mesophyll cells, while the reference electrode was placed in the bath solution. (b, c) Representative membrane potential traces of mesophyll cells exposed to 1000 ppb O_3 for 3 and 10 min, respectively. Ozone exposure period is indicated with blue lines. The bar below the graphs indicates if the leaf was exposed to light or kept in the darkness. The *x*-axis displays the time relative to the start of O_3 application. Both treatment regime experiments were repeated at least seven times with similar results. (d) Three phases in the membrane potential response to O_3 observed at the beginning of both 3- and 10-min O_3 treatments: (1) initial depolarization that starts almost immediately upon application of O_3 (2) second steep, but transient, depolarization (3) sustained depolarization.

response was attenuated compared to the 3 min O_3 experiment (Fig. 2b). Application of the same volume of pure oxygen as the volume of airflow added during O_3 exposure led to no change in the membrane potential (Fig. S3).

In all measured cells, the O_3-induced early membrane potential response displayed three distinct phases (Fig. 2d; Table S1). Within 1–2 s after O_3 application a small depolarization ($\Delta V = 4.5$ mV, SEM = 0.4, $n = 25$) occurred that lasted on average for 23 s (SEM = 1.1). This early response was followed by a stronger depolarization that had a distinct peak ($\Delta V = 27.5$ mV, SEM = 2.4, $n = 25$) on average at 42 s (SEM = 3.2), after the onset of the stimulus. In phase 3 a slow further depolarization was evident after which membrane potential slightly repolarized. On average, the maximum change in membrane potential during these three phases was 47 mV (SEM = 3.2) that was reached 134 s (SEM = 25.9) after the start of the exposure.

Ozone induces cytosolic calcium signals in mesophyll and vascular cells

Stress responses in plant cells are often accompanied by cytosolic calcium signals, which can activate plasma membrane anion channels that in turn cause a depolarization (Barbier-Brygoo *et al.*, 2011; Roelfsema *et al.*, 2012). We therefore studied changes in cytosolic calcium level with RG-mT, a genetically encoded dual-wavelength calcium reporter (Waadt *et al.*, 2017). RG-mT fluorescence and membrane potential (E_m) values were measured simultaneously before, during, and after a 10-min pulse of 1000 ppb of O_3 (Video S1). Ozone-induced changes in cytosolic [Ca^{2+}] and membrane potential (E_m) showed a similar pattern, characterized by a fast increase of RG-mT fluorescence ratio and a depolarization in the first 2 min, thereafter both values recovered, followed by a second increase of the RG-mT signal

and a depolarization (Fig. 3a,b). However, in comparison to the change in E_m, the RG-mT fluorescence did not exhibit a fast peak during the first depolarization (phase 1 in Fig. 2d) and reached its peak value slightly later as the maximum depolarization (Fig. 3b).

The timing and nature of the O_3-induced membrane depolarization and cytosolic [Ca^{2+}] increases were analysed in further detail, by application of several concentrations of O_3. Lowering the O_3 concentration from 1000 to 600 and 200 ppb decreased the magnitude of the depolarization, but the timing remained virtually unchanged (Figs 3c, S4). A similar O_3 concentration dependence was found for the calcium response, recorded with R-GECO1 (Fig. 3d). However, the calcium level remained constant during the first phase of the E_m-response, directly after application of O_3 (Fig. 3d), just as described earlier for Fig. 3(b).

We compared the O_3-induced Ca^{2+} responses of cells in the veins and those located in the intercostal fields, which were stimulated with two consecutive 1000 ppb O_3 pulses (Fig. 4). The RG-mT signal showed a strong increase in the intercostal fields and a much lower change in the veins during the first O_3 pulse, while during the second O_3 exposure, the Ca^{2+}-increase in the veins was delayed in comparison to the intercostal fields. This suggests that cells in intercostal fields are more responsive, most likely because O_3 first enters the intercellular air space through stomata in this region, while its concentration decreases when it travels towards the veins within the leaf disc.

Hydrogen peroxide activates calcium ion-permeable channels and depolarizes mesophyll cells

Upon entrance into leaves, O_3 will form several ROS including H_2O_2, which was previously shown to activate non-selective cation channels in various cell types (Pei *et al.*, 2000a; Demidchik *et al.*, 2003). We therefore tested if mesophyll cells possess such Ca^{2+}-permeable channels, using the patch clamp technique with mesophyll protoplast of *Arabidopsis* (Fig. 5a). Application of H_2O_2 lead to an increase of inward current that is typical for Ca^{2+} permeable cation channels, under the experimental conditions used (Stoelzle *et al.*, 2003) (Fig. 5b,c). These channels are thus good candidates to facilitate the O_3-induced rise of the cytosolic Ca^{2+} concentration. High cytosolic Ca^{2+} concentrations can activate plant anion channels (Geiger *et al.*, 2010; Scherzer *et al.*, 2012), including those of mesophyll cells of pea plants (Elzenga & Van Volkenburgh, 1997), which will lead to a depolarization at physiological relevant conditions (Roelfsema *et al.*, 2012). In line with this sequence of events, application of H_2O_2 depolarized mesophyll cells in a concentration-dependent manner (Fig. 5d,e). However, the H_2O_2-induced depolarization differed from that provoked by O_3, as the H_2O_2 response lacked the initial depolarization (phase I in Fig. 2d) and the transient nature, which was observed after application of O_3 (Fig. 2b,c).

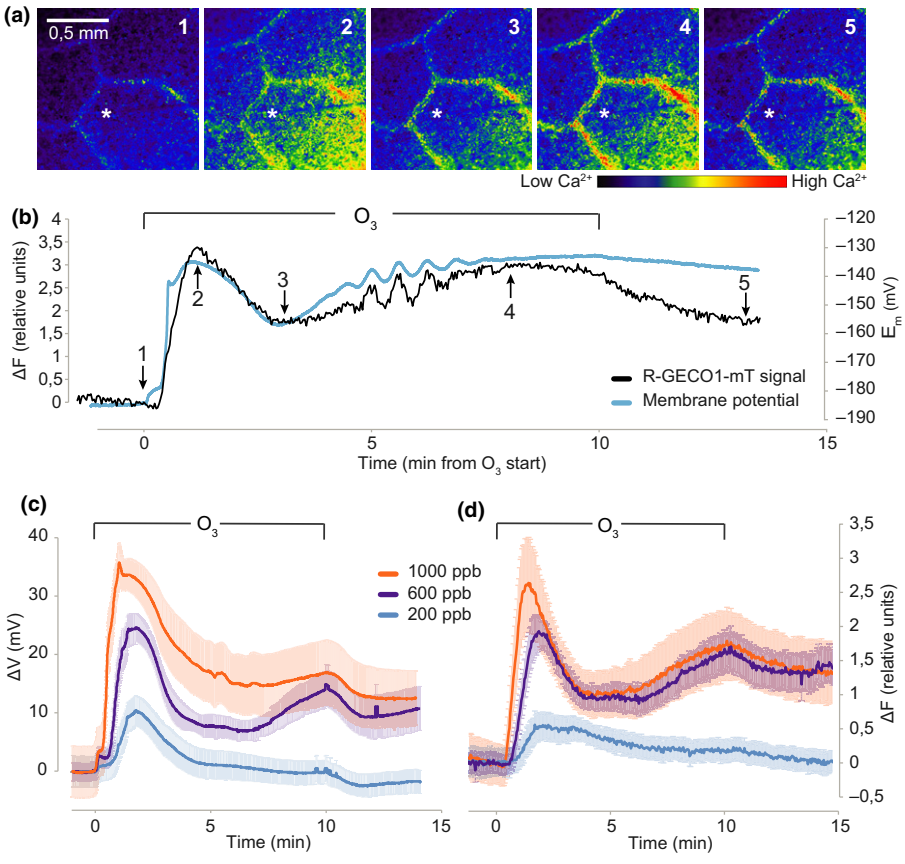

Fig. 3 Effect of ozone (O_3) on mesophyll cells' cytosolic calcium level. (a) Pseudo-colour images of the R-GECO1 fluorescence intensity of an *Arabidopsis* leaf disc, exposed for 10 min to 1000 ppb O_3, starting in image 2. Numbers on the images indicate the acquisition timepoint and correspond to (b). The horizontal line visible in the middle of the image is the measurement electrode, the location of its tip is marked with an asterisk. (b) A representative measurement of simultaneous recording of the RG-mT fluorescence ratio in the leaf disc, and membrane potential of a mesophyll cell (E_m). The time period of O_3 (1000 ppb) application is indicated above the graph; numbers correspond to the images in (a). (c, d) Simultaneous measurements of E_m and RG-mT fluorescence in leaf discs stimulated with pulses of 200, 600 and 1000 ppb O_3. The stimuli were applied at timepoint 0 for 10 min. (c) The E_m changes (ΔV) in response to O_3, relative to the average E_m values during 30 s before application of the stimulus; (d) R-GECO1/mT ratio change, relative to the average value during 30 s before O_3 exposure. $n = 9–12$, error bars represent SEM.

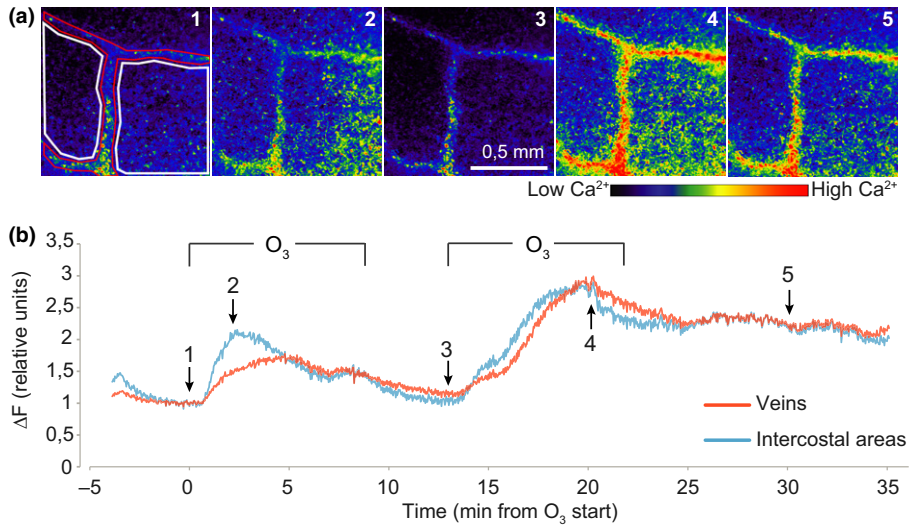

Fig. 4 Ozone (O_3) evokes repetitive cytosolic calcium increases in *Arabidopsis* leaf cells. (a) Pseudo-colour images indicating the R-GECO1 fluorescence intensity, from a leaf disc that was stimulated with two pulses of O_3; 1000 ppb O_3 was applied in between 1 and 2 as well as between 3 and 4. Numbers correspond to the timepoints indicated in (b). Regions of interests used for analysis are outlined on the first image in red (veins) and white (intercostal areas). (b) Two pulses of 1000 ppb O_3 were applied to a leaf disc, as indicated above the graph. Changes in the R-GECO1 fluorescence intensity are given relative to the average value 30 s before the first exposure. Changes in R-GECO1 fluorescence were calculated separately for the leaf bundles (veins) and the areas between them (intercostal areas). The experiment was repeated seven times with similar results.

Ozone-induced calcium response spreads to neighbouring cells only at concentrations that trigger cell death

As ROS have been demonstrated to trigger long-distance calcium waves (Evans *et al.*, 2016), we studied if O_3-induced calcium signals are transmitted to leaf areas that are not in direct contact with the stimulus. Part of the leaf was covered with a thin layer of agarose gel, which reduced the flow of O_3 reaching the leaf more than 99% (Fig. S1). The rest of the leaf remained uncovered and could thus be stimulated with O_3. Two successive O_3 pulses were applied, a first one with 1000 ppb and 10 min later a second with 5000 ppb. The first exposure to 1000 ppb O_3 evoked a transient increase in the calcium level in the uncovered area, but no calcium signal was recorded in the covered area (Fig. 6; Video S2). However, application of a five-times higher O_3 concentration (5000 ppb) triggered calcium signals both in the uncovered as well as covered area (Fig. 6). The latter calcium response started with a delay and was most apparent in the area closest to the part of the leaf that was in contact with the atmosphere. A strong O_3 pulse of 5000 ppb thus appears to induce a calcium wave that travels from cells that are directly stimulated with O_3 to tissues that were covered by agarose (Video S2).

The induction of Ca^{2+} waves by strong O_3 pulses (5000 ppb) indicates activation of a different process in comparison to the local increase in Ca^{2+} triggered by a lower O_3 concentration (1000 ppb). The response to 5000 ppb was therefore studied in further detail with gas-exchange experiments, which showed that 3 min of 5000 ppb O_3 caused a sustained decrease of the stomatal conductance, as well as the CO_2 uptake rate (Fig. 7a,b). Note that both the stomatal conductance and CO_2 assimilation both fully recovered after a pulse of 1000 ppb (Fig. 1a). Pulses of 5000 ppb thus seem to cause an irreversible damage to the leaves, which leads to a very low stomatal conductance (Fig. 7a). The latter response is probably linked to the cell death that became visible in the following days (Figs 7c, S2b).

Discussion

Three phases of the early membrane response to ozone

This study provides insights into the earliest O_3-triggered ROS signalling events in mesophyll cells. We recorded a sequence of changes in the membrane potential and cytosolic Ca^{2+} level that were induced within a few seconds and could be separated into three phases.

In the first phase, the membrane depolarizes slightly, but no change in the cytosolic calcium level can be observed yet (Figs 2, 3). It is probable that a plasma membrane Ca^{2+} permeable conductance is activated in this phase, which causes the initial small depolarization, but the changes in the cytosolic Ca^{2+} level are not yet strong enough to be detected with the R-GECO1 reporter. The ROS-activated Ca^{2+}-permeable cation channel that was detected with the patch clamp technique (Fig. 5b,c) is a good candidate to contribute to this initial depolarization. Similar ROS-activated Ca^{2+}-permeable channels have been identified in various cells (Pei *et al.*, 2000b; Demidchik *et al.*, 2003, 2018), but their molecular nature still not resolved. These channels may be encoded by genes belonging to the families of hyperosmolality-gated calcium-permeable channels (OSCA) (Yuan *et al.*, 2014) and cyclic nucleotide gated channels (CNGC) (DeFalco *et al.*, 2016), however, further research will be required to clarify this issue.

During the second and third phase of the O_3 response (Fig. 3b), the changes in cytosolic Ca^{2+} concentration and the

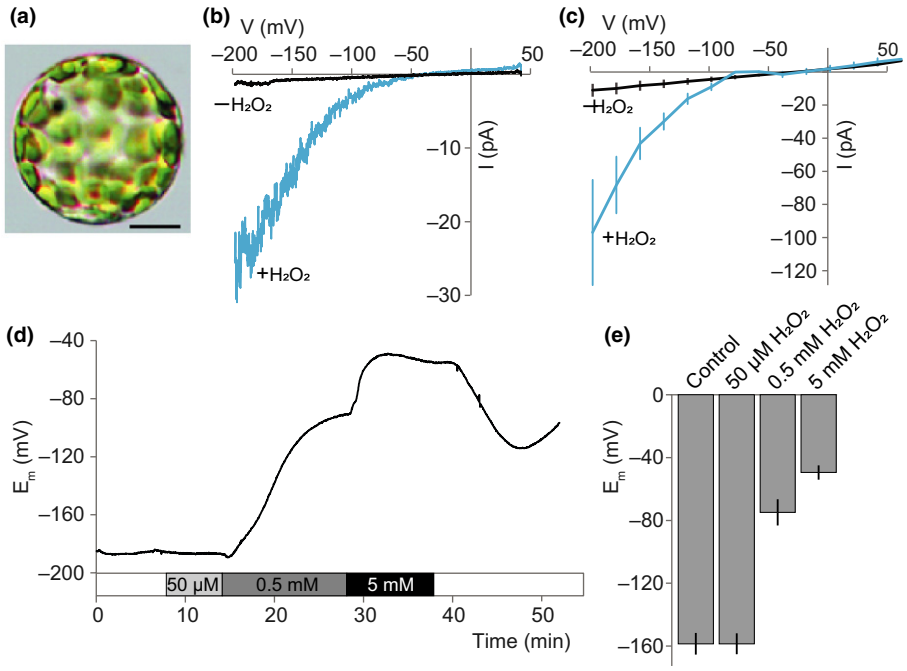

Fig. 5 Hydrogen peroxide (H_2O_2) activates calcium-permeable channels in mesophyll cells and triggers a depolarization. (a) Image of an enzymatically isolated mesophyll *Arabidopsis* protoplast (scale bar = 10 µm). (b) Current traces in response to voltage ramps before and after application of 5 mM H_2O_2 to the bath solution. (c) Mean steady-state currents determined from voltage pulse experiments in the absence and presence of 5 mM H_2O_2, in the cell-attached configuration. $n = 5$, error bars represent SEM. (d) Membrane potential of mesophyll cells exposed to control solution (white area in bar below the graph), 50 µM H_2O_2 (light grey area in bar), 0.5 mM H_2O_2 (dark grey area in bar) and 5 mM H_2O_2 (black area in bar). (e) Average membrane potentials of mesophyll cells measured at control conditions, or at H_2O_2 concentrations as indicated above the graph. $n = 9$–11, errors bars represent SEM.

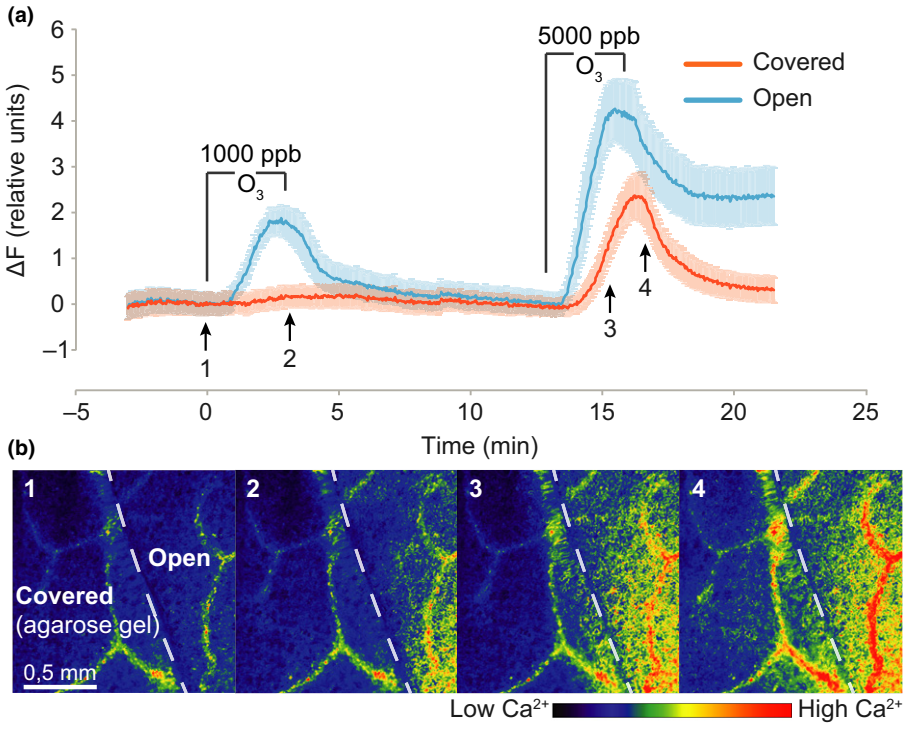

Fig. 6 Ozone (O_3) pulses of 5000 ppb provoke long-distance calcium ion (Ca^{2+}) signals. (a) R-GECO1/mT ratio change in *Arabidopsis thaliana* leaf discs exposed to two 3-min pulses of O_3 of 1000 ppb (first pulse) and 5000 ppb (second pulse). Half of the leaf area in the field of view was in contact with the air flow (blue trace), while the other half was covered with a thin layer of agarose gel (red trace). Note that the Ca^{2+} signal does not continue in the covered area of the leaf during stimulation with 1000 ppb, while 5000 ppb causes a long-distance Ca^{2+} signal. $n = 8$, error bars represent SEM. (b) Pseudo-colour images of the R-GECO1 fluorescence intensity in a leaf disc exposed to two pulses of O_3 as in (a), numbers correspond. Dashed line indicates the rim of the agarose gel covering the left part of the leaf disc.

plasma membrane potential go hand in hand. Such a close correlation between increasing cytosolic Ca^{2+} and the membrane potential was also found for guard cells of tobacco (Chen *et al.*, 2010; Stange *et al.*, 2010) and *Arabidopsis* (Huang *et al.*, 2019). In guard cells, the SLAC1 and SLAH3 anion channels are activated by an increase in cytosolic calcium concentration and a calcium-activated anion channel has also been identified in mesophyll cells of pea (Elzenga & Van Volkenburgh, 1997). Elevation of the cytosolic Ca^{2+} concentration in mesophyll cells thus may lead to activation of plasma membrane anion channels, which in turn will cause a depolarization of the plasma membrane. The SLAH3 anion channel is expressed in mesophyll cells (Geiger *et al.*, 2011; Demir *et al.*, 2013) and future research may reveal if this channel and/or other anion channels cause the transient depolarization in phase 2.

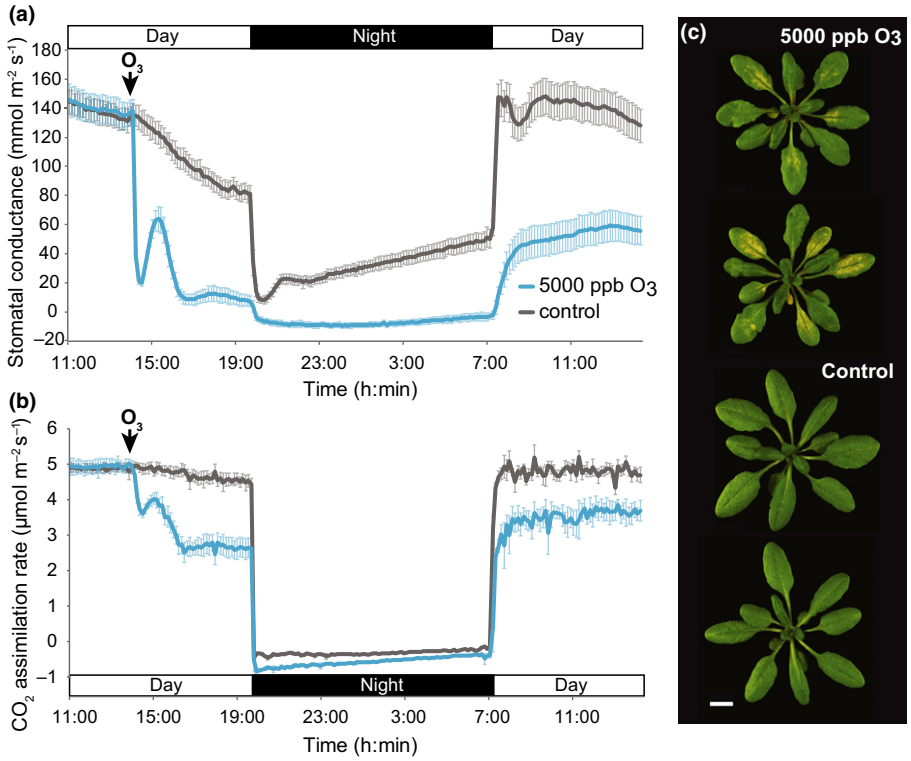

Fig. 7 Ozone (O_3) pulses of 5000 ppb cause irreversible damage to 4-wk-old *Arabidopsis* plants. (a, b) Impact of a pulse of 3 min of 5000 ppb of O_3 on the stomatal conductance (a) and CO_2 uptake rate (b). Results from one experiment are shown. $n = 4$, error bars represent SEM. (c) Representative images of plants subjected to 3 min 5000 ppb O_3 and control plants 72 h after treatment. Scale bar represents 1 cm.

A drop in photosynthetic CO_2 assimilation precedes stomatal closure

Ozone caused an early drop in CO_2 assimilation that occurred even before stomata started to close (Fig. 2b). It is not likely that photosynthesis was restricted by the stomatal conductance, as stomata started closing later than CO_2 assimilation began to decrease. Instead, the reduced assimilation may be due to a decreased activity of Rubisco, or damage to photosystem II. These targets have been identified in experiments with chronic O_3 exposure (Calatayud *et al.*, 2003; Morgan *et al.*, 2003; Goumenaki *et al.*, 2010; Feng *et al.*, 2016) and acute O_3 stimuli (up to 500 ppb of O_3 for several hours) (Leipner *et al.*, 2001; Chen *et al.*, 2009; Morales *et al.*, 2021). The observed reduction in CO_2 assimilation, in response to 1000 ppb of O_3 within 1 min (Fig. 1d), is remarkably fast and future studies may reveal if this is caused by the direct damage to photosynthetic apparatus within such a short timeframe, or possibly by a signal that is evoked at the plasma membrane and rapidly transmitted to the chloroplasts. Possibly, the fast increase in the cytosolic Ca^{2+} level, which occurs in seconds after O_3 application is sensed by the chloroplasts. Moreover, further experiments are needed to address if the fast response in mesophyll CO_2 assimilation occurs before, or simultaneously with the earliest responses in guard cells and if mesophyll cells may forward the O_3 signal to the stomata.

Two types of ozone-induced calcium ion signals

Mesophyll cells responded rapidly to O_3 at concentrations as low as 200 ppb (Fig. 3), however concentrations up to 1000 ppb neither lead to visible damage, nor to a drop in CO_2 assimilation that would persist for more than a day (Figs 1b, S2a). These O_3 doses also cause Ca^{2+}-signals in cells that are directly in contact with O_3, but not in the adjacent tissue. In contrast, exposure to 5000 ppb O_3 did lead to cell death and provoked a spreading response in distant cells, which is characterized by long distance systemic Ca^{2+}-signals.

Our results bare similarities to those of Kiep *et al.* (2015), who studied *Spodoptera littoralis* larvae feeding on *Arabidopsis* leaves. Feeding caused a confined calcium rise, as long as the larvae did not damage the midrib of the leaf (Kiep *et al.*, 2015). However, injury of the midrib caused a strong systemic signal that was linked to a long distance Ca^{2+} wave. These data thus suggest that plants discriminate between the location and/or strength of stress stimuli. Stress responses are restricted to local responses, as long as the stimuli do not provoke cell death. However, strong stress responses that are linked to cell death are fed forward and initiate Ca^{2+} waves that travel along the vasculature and spread within the adjacent mesophyll tissue (Toyota *et al.*, 2018). Our data thus show that leaf cells are exceptionally sensitive to stress-related signals and discriminate between the strength of the stimulus with local responses at low doses and spreading responses that cause cell death at a higher dose of O_3.

Acknowledgements

The support of the German Science Foundation (DFG), projects HE1640/40-1 and RO2381/8-1, awarded to RH and MRGR, and of the Estonian Ministry of Science and Education (PRG433) and European Regional Development Fund (Centre of Excellence in Molecular Cell Engineering (CEMCE)) to HK is gratefully acknowledged.

Author contributions

MN, MB, PD, RH, MRGR and HK planned and designed the research. MN, SS-F and MRGR performed experiments and analysed data. MN, MRGR and HK wrote the manuscript with comments and inputs from all authors.

ORCID

Mikael Brosché https://orcid.org/0000-0002-1135-2496
Petra Dietrich https://orcid.org/0000-0002-9209-8089
Rainer Hedrich https://orcid.org/0000-0003-3224-1362
Hannes Kollist https://orcid.org/0000-0002-6895-3583
Maris Nuhkat https://orcid.org/0000-0002-8001-4220
M. Rob G. Roelfsema https://orcid.org/0000-0002-4076-4246
Sonja Stoelzle-Feix https://orcid.org/0000-0002-3847-7491

Data availability

The data that support the findings of this study are available from the corresponding author upon reasonable request.

References

Barbier-Brygoo H, De Angeli A, Filleur S, Frachisse J-M, Gambale F, Thomine S, Wege S. 2011. Anion channels/transporters in plants: from molecular bases to regulatory networks. *Annual Review of Plant Biology* **62**: 25–51.

Blatt M, Armstrong F. 1993. K^+ channels of stomatal guard cells: abscisic-acid-evoked control of the outward rectifier mediated by cytoplasmic pH. *Planta* **191**: 330–341.

Calatayud A, Iglesias DJ, Talón M, Barreno E. 2003. Effects of 2-month ozone exposure in spinach leaves on photosynthesis, antioxidant systems and lipid peroxidation. *Plant Physiology and Biochemistry* **41**: 839–845.

Chen CP, Frank TD, Long SP. 2009. Is a short, sharp shock equivalent to long-term punishment? Contrasting the spatial pattern of acute and chronic ozone damage to soybean leaves via chlorophyll fluorescence imaging. *Plant, Cell & Environment* **32**: 327–335.

Chen ZH, Hills A, Lim CK, Blatt MR. 2010. Dynamic regulation of guard cell anion channels by cytosolic free Ca^{2+} concentration and protein phosphorylation. *The Plant Journal* **61**: 816–825.

Clayton H, Knight MR, Knight H, McAinsh MR, Hetherington AM. 1999. Dissection of the ozone-induced calcium signature. *The Plant Journal* **17**: 575–579.

Colcombet J, Mathieu Y, Peyronnet R, Agier N, Lelièvre F, Barbier-Brygoo H, Frachisse JM. 2009. R-type anion channel activation is an essential step for ROS-dependent innate immune response in *Arabidopsis* suspension cells. *Functional Plant Biology* **36**: 832–843.

DeFalco TA, Moeder W, Yoshioka K. 2016. Opening the gates: insights into cyclic nucleotide-gated channel-mediated signaling. *Trends in Plant Science* **21**: 903–906.

Demidchik V, Cuin TA, Svistunenko D, Smith SJ, Miller AJ, Shabala S, Sokolik A, Yurin V. 2010. *Arabidopsis* root K^+-efflux conductance activated by hydroxyl radicals: single-channel properties, genetic basis and involvement in stress-induced cell death. *Journal of Cell Science* **123**: 1468–1479.

Demidchik V, Shabala SN, Coutts KB, Tester MA, Davies JM. 2003. Free oxygen radicals regulate plasma membrane Ca^{2+}- and K^+-permeable channels in plant root cells. *Journal of Cell Science* **116**: 81–88.

Demidchik V, Shabala S, Isayenkov S, Cuin TA, Pottosin I. 2018. Calcium transport across plant membranes: mechanisms and functions. *New Phytologist* **220**: 49–69.

Demir F, Horntrich C, Blachutzik JO, Scherzer S, Reinders Y, Kierszniowska S, Schulze WX, Harms GS, Hedrich R, Geiger D *et al.* 2013. Arabidopsis nanodomain-delimited ABA signaling pathway regulates the anion channel SLAH3. *Proceedings of the National Academy of Sciences, USA* **110**: 8296–8301.

Dunand C, Crèvecoeur M, Penel C. 2007. Distribution of superoxide and hydrogen peroxide in *Arabidopsis* root and their influence on root development: possible interaction with peroxidases. *New Phytologist* **174**: 332–341.

El-Maarouf H, Barny MA, Rona JP, Bouteau F. 2001. Harpin, a hypersensitive response elicitor from *Erwinia amylovora*, regulates ion channel activities in *Arabidopsis thaliana* suspension cells. *FEBS Letters* **497**: 82–84.

Elzenga JTM, Prins HBA, Van Volkenburgh E. 1995. Light-induced membrane potential changes of epidermal and mesophyll cells in growing leaves of *Pisum sativum*. *Planta* **197**: 127–134.

Elzenga JTM, Van Volkenburgh E. 1997. Characterization of a light-controlled anion channel in the plasma membrane of mesophyll cells of pea. *Plant Physiology* **113**: 1419–1426.

Evans MJ, Choi WG, Gilroy S, Morris RJ. 2016. A ROS-assisted calcium wave dependent on the AtRBOHD NADPH oxidase and TPC1 cation channel propagates the systemic response to salt stress. *Plant Physiology* **171**: 1771–1784.

Evans NH, McAinsh MR, Hetherington AM, Knight MR. 2005. ROS perception in *Arabidopsis thaliana*: the ozone-induced calcium response. *The Plant Journal* **41**: 615–626.

Feng Z, Wang L, Pleijel H, Zhu J, Kobayashi K. 2016. Differential effects of ozone on photosynthesis of winter wheat among cultivars depend on antioxidative enzymes rather than stomatal conductance. *Science of the Total Environment* **572**: 404–411.

Geiger D, Maierhofer T, AL-Rasheid KAS, Scherzer S, Mumm P, Liese A, Ache P, Wellmann C, Marten I, Grill E *et al.* 2011. Stomatal closure by fast abscisic acid signaling is mediated by the guard cell anion channel SLAH3 and the receptor RCAR1. *Science Signaling* **4**: ra32.

Geiger D, Scherzer S, Mumm P, Marten I, Ache P, Matschi S, Liese A, Wellmann C, Al-Rasheid KAS, Grill E *et al.* 2010. Guard cell anion channel SLAC1 is regulated by CDPK protein kinases with distinct Ca^{2+} affinities. *Proceedings of the National Academy of Sciences, USA* **107**: 8023–8028.

Goumenaki E, Taybi T, Borland A, Barnes J. 2010. Mechanisms underlying the impacts of ozone on photosynthetic performance. *Environmental and Experimental Botany* **69**: 259–266.

Grabov A, Blatt MR. 1999. A steep dependence of inward-rectifying potassium channels on cytosolic free calcium concentration increase evoked by hyperpolarization in guard cells. *Plant Physiology* **119**: 277–287.

Grimes HD, Perkins KK, Boss WF. 1983. Ozone degrades into hydroxyl radical under physiological conditions. A spin trapping study. *Plant Physiology* **72**: 1016–1020.

Halliwell B. 2006. Reactive species and antioxidants. Redox biology is a fundamental theme of aerobic life. *Plant Physiology* **141**: 312–322.

Huang S, Waadt R, Nuhkat M, Kollist H, Hedrich R, Roelfsema MRG. 2019. Calcium signals in guard cells enhance the efficiency by which abscisic acid triggers stomatal closure. *New Phytologist* **224**: 177–187.

Jeworutzki E, Roelfsema MRG, Anschütz U, Krol E, Elzenga JTM, Felix G, Boller T, Hedrich R, Becker D. 2010. Early signaling through the *Arabidopsis* pattern recognition receptors FLS2 and EFR involves Ca^{2+}-associated opening of plasma membrane anion channels. *The Plant Journal* **62**: 367–378.

Kadono T, Tran D, Errakhi R, Hiramatsu T, Meimoun P, Briand J, Iwaya-Inoue M, Kawano T, Bouteau F. 2010. Increased anion channel activity is an unavoidable event in ozone-induced programmed cell death. *PLoS ONE* **5**: e13373.

Kadono T, Yamaguchi Y, Furuichi T, Hirono M, Garrec JP, Kawano T. 2006. Ozone-induced cell death mediated with oxidative and calcium signaling pathways in tobacco Bel-W3 and Bel-B cell suspension cultures. *Plant Signaling and Behavior* **1**: 312–322.

Kadota Y, Shirasu K, Zipfel C. 2015. Regulation of the NADPH oxidase RBOHD during plant immunity. *Plant and Cell Physiology* **56**: 1472–1480.

Kangasjärvi J, Jaspers P, Kollist H. 2005. Signalling and cell death in ozone-exposed plants. *Plant, Cell & Environment* **28**: 1021–1036.

Kanofsky JR, Sima PD. 1995. Singlet oxygen generation from the reaction of ozone with plant leaves. *Journal of Biological Chemistry* **270**: 7850–7852.

Keinath NF, Waadt R, Brugman R, Schroeder JI, Grossmann G, Schumacher K, Krebs M. 2015. Live cell imaging with R-GECO1 sheds light on flg22- and chitin-induced transient $[Ca^{2+}]_{cyt}$ patterns in *Arabidopsis*. *Molecular Plant* **8**: 1188–1200.

Kiep V, Vadassery J, Lattke J, Maaß JP, Boland W, Peiter E, Mithöfer A. 2015. Systemic cytosolic Ca^{2+} elevation is activated upon wounding and herbivory in *Arabidopsis*. *New Phytologist* **207**: 996–1004.

Kollist T, Moldau H, Rasulov B, Oja V, Rämma H, Hüve K, Jaspers P, Kangasjärvi J, Kollist H. 2007. A novel device detects a rapid ozone-induced transient stomatal closure in intact *Arabidopsis* and its absence in abi2 mutant. *Physiologia Plantarum* **129**: 796–803.

Leipner J, Oxborough K, Baker NR. 2001. Primary sites of ozone-induced perturbations of photosynthesis in leaves: identification and characterization in *Phaseolus vulgaris* using high resolution chlorophyll fluorescence imaging. *Journal of Experimental Botany* **52**: 1689–1696.

Mittler R. 2017. ROS are good. *Trends in Plant Science* **22**: 11–19.

Moldau H. 1998. Hierarchy of ozone scavenging reactions in the plant cell wall. *Physiologia Plantarum* **104**: 617–622.

Morales LO, Shapiguzov A, Safronov O, Leppälä J, Vaahtera L, Yarmolinsky D, Kollist H, Brosché M. 2021. Ozone responses in *Arabidopsis*: beyond stomatal conductance. *Plant Physiology* **186**: 180–192.

Morgan PB, Ainsworth EA, Long SP. 2003. How does elevated ozone impact soybean? A meta-analysis of photosynthesis, growth and yield. *Plant, Cell & Environment* **26**: 1317–1328.

Pei ZM, Murata Y, Benning G, Thomine S, Klüsener B, Allen GJ, Grill E, Schroeder JI. 2000a. Calcium channels activated by hydrogen peroxide mediate abscisic acid signalling in guard cells. *Nature* **406**: 731–734.

Pei ZM, Murata Y, Benning G, Thomine S, Klüsener B, Allen GJ, Grill E, Schroeder JI. 2000b. Calcium channels activated by hydrogen peroxide mediate abscisic acid signalling in guard cells. *Nature* **406**: 731–734.

Roelfsema MRG, Hedrich R, Geiger D. 2012. Anion channels: master switches of stress responses. *Trends in Plant Science* **17**: 221–229.

Scherzer S, Maierhofer T, Al-Rasheid KAS, Geiger D, Hedrich R. 2012. Multiple calcium-dependent kinases modulate ABA-activated guard cell anion channels. *Molecular Plant* **5**: 1409–1412.

Schneider CA, Rasband WS, Eliceiri KW. 2012. NIH image to ImageJ: 25 years of image analysis. *Nature Methods* **9**: 671–675.

Short EF, North KA, Roberts MR, Hetherington AM, Shirras AD, McAinsh MR. 2012. A stress-specific calcium signature regulating an ozone-responsive gene expression network in *Arabidopsis*. *The Plant Journal* **71**: 948–961.

Sierla M, Waszczak C, Vahisalu T, Kangasjärvi J. 2016. Reactive oxygen species in the regulation of stomatal movements. *Plant Physiology* **171**: 1569–1580.

von Sonntag C, von Gunten U. 2012. *Chemistry of ozone in water and wastewater treatment: from basic principles to applications*. London, UK: IWA Publishing.

Stange A, Hedrich R, Roelfsema MRG. 2010. Ca^{2+}-dependent **activation of guard cell anion channels, triggered by hyperpolarization, is promoted by prolonged depolarization.** *The Plant Journal* **62**: 265–276.

Stoelzle S, Kagawa T, Wada M, Hedrich R, Dietrich P. 2003. Blue light activates calcium-permeable channels in *Arabidopsis* mesophyll cells via the phototropin signaling pathway. *Proceedings of the National Academy of Sciences, USA* **100**: 1456–1461.

Torsethaugen G, Pell EJ, Assmann SM. 1999. Ozone inhibits guard cell K^+ channels implicated in stomatal opening. *Proceedings of the National Academy of Sciences, USA* **96**: 13577–13582.

Toyota M, Spencer D, Sawai-Toyota S, Jiaqi W, Zhang T, Koo AJ, Howe GA, Gilroy S. 2018. Glutamate triggers long-distance, calcium-based plant defense signaling. *Science* **361**: 1112–1115.

Tran D, El-Maarouf-Bouteau H, Rossi M, Biligui B, Briand J, Kawano T, Mancuso S, Bouteau F. 2013. Post-transcriptional regulation of GORK channels by superoxide anion contributes to increases in outward-rectifying K^+ currents. *New Phytologist* **198**: 1039–1048.

Tsukagoshi H, Busch W, Benfey PN. 2010. Transcriptional regulation of ROS controls transition from proliferation to differentiation in the root. *Cell* **143**: 606–616.

Vahisalu T, Puzõrjova I, Brosché M, Valk E, Lepiku M, Moldau H, Pechter P, Wang Y-S, Lindgren O, Salojärvi J *et al.* 2010. Ozone-triggered rapid stomatal response involves the production of reactive oxygen species, and is controlled by SLAC1 and OST1. *The Plant Journal* **62**: 442–453.

Vaultier MN, Jolivet Y. 2015. Ozone sensing and early signaling in plants: an outline from the cloud. *Environmental and Experimental Botany* **114**: 144–152.

Waadt R, Krebs M, Kudla J, Schumacher K. 2017. Multiparameter imaging of calcium and abscisic acid and high-resolution quantitative calcium measurements using R-GECO1-mTurquoise in *Arabidopsis*. *New Phytologist* **216**: 303–320.

Waszczak C, Carmody M, Kangasjärvi J. 2018. Reactive oxygen species in plant signaling. *Annual Review of Plant Biology* **69**: 209–236.

Wendehenne D, Lamotte O, Frachisse JM, Barbier-Brygoo H, Pugin A. 2002. Nitrate efflux is an essential component of the cryptogein signaling pathway leading to defense responses and hypersensitive cell death in tobacco. *Plant Cell* **14**: 1937–1951.

Wohlgemuth H, Mittelstrass K, Kschieschan S, Bender J, Weigel HJ, Overmyer K, Kangasjärvi J, Sandermann H, Langebartels C. 2002. Activation of an oxidative burst is a general feature of sensitive plants exposed to the air pollutant ozone. *Plant, Cell & Environment* **25**: 717–726.

Wong-Ekkabut J, Xu Z, Triampo W, Tang IM, Tieleman DP, Monticelli L. 2007. Effect of lipid peroxidation on the properties of lipid bilayers: a molecular dynamics study. *Biophysical Journal* **93**: 4225–4236.

Wu F, Chi Y, Jiang Z, Xu Y, Xie L, Huang F, Wan DI, Ni J, Yuan F, Wu X *et al.* 2020. Hydrogen peroxide sensor HPCA1 is an LRR receptor kinase in *Arabidopsis*. *Nature* **578**: 577–581.

Yuan F, Yang H, Xue Y, Kong D, Ye R, Li C, Zhang J, Theprungsirikul L, Shrift T, Krichilsky B *et al.* 2014. OSCA1 mediates osmotic-stress-evoked Ca^{2+} increases vital for osmosensing in *Arabidopsis*. *Nature* **514**: 367–371.

Supporting Information

Additional Supporting Information may be found online in the Supporting Information section at the end of the article.

Fig. S1 The effect of agarose gel on ozone diffusion.

Fig. S2 Visible symptoms in *Arabidopsis* plants in response to 1000 and 5000 ppb ozone.

Fig. S3 Oxygen and ozone-induced changes in the membrane potential of *Arabidopsis* mesophyll cells.

Fig. S4 Effect of different concentrations of ozone on mesophyll cells' membrane potential and leaf discs' R-GECO1/mT fluorescence.

Table S1 Average membrane potential values of mesophyll cells stimulated with air that contained 1000 ppb ozone (see Fig. 2 for representative E_m traces).

Video S1 R-GECO1 signal change in leaf tissue during ozone exposure.

Video S2 R-GECO1 signal change in leaf tissue during ozone pulses of 1000 ppb and 5000 ppb.

Please note: Wiley Blackwell are not responsible for the content or functionality of any Supporting Information supplied by the authors. Any queries (other than missing material) should be directed to the *New Phytologist* Central Office.